This is a repository copy of *On the Transient Decomposition and Reaction Kinetics of Zinc Dialkyldithiophosphate*.

Article:

Dorgham, A, Azam, A orcid.org/0000-0002-3510-1333, Morina, A orcid.org/0000-0001-8868-2664 et al. (1 more author) (2018) On the Transient Decomposition and Reaction Kinetics of Zinc Dialkyldithiophosphate. ACS Applied Materials and Interfaces, 10 (51). pp. 44803-44814. ISSN 1944-8244

https://doi.org/10.1021/acsami.8b08293

On the Transient Decomposition and Reaction Kinetics of Zinc Dialkyldithiophosphate

Abdel Dorgham*, Abdullah Azam, Ardian Morina and Anne Neville

Institute of Functional Surfaces, School of Mechanical Engineering, University of Leeds, Leeds LS2 9JT, United Kingdom

Abstract: Despite the ubiquitous use of the zinc dialkyldithiophosphate (ZDDP) as antiwear additive, no complete information is yet available on its exact decomposition reactions and kinetics to form triboreactive protective films on contacting surfaces. This hinders the replacement of ZDDP with more environmental friendly additives of similar antiwear capabilities. Using a multi-technique approach, this study shows that before the formation of a phosphate-rich protective film, the decomposition of ZDDP proceeds by forming intermediate zinc sulfide and sulfate species, which can be mechanically mixed with the iron oxides on the rubbing steel surfaces. The mixed sulfur-oxide layer can play different vital roles including binding the subsequently formed phosphate layers with the metal surface. These layers consist mainly of zinc thiophosphate of initially short chains, which are formed due to the excess concentration of metal oxide on the surface. As the concentration of the oxide decreases in the subsequent layers, the short chains start to polymerize into longer ones. The polymerization process follows first-order reaction kinetics with two distinctive phases. The first one is a fast transient burst phase near the steel surface, whereas the second phase dominates the formation process of the layers away from the substrate and is characterized by slow kinetics. The findings of this study provide new insights into the decomposition mechanisms of the currently most widely used antiwear additive and open future opportunities to find green alternatives with similar superior antiwear properties.

Keywords: *ZDDP, reaction kinetics, antiwear tribofilm, wear, tribology*

Introduction

Over the last 70 years, different theories were proposed to explain the ZDDP decomposition reactions to form protective triboreactive films, called tribofilms, covering the contacting surfaces. These works were discussed in different reviews.[1–3] However, despite being studied extensively, little is known about the exact kinetics of the ZDDP decomposition reactions. This is mainly because they are tribo-induced, which can follow different complex pathways. In addition, the commercial oils containing ZDDP may also contain some impurities, other additives, detergents or dispersants that might alter these pathways and ultimately alter the precursors and the final reaction products, i.e. the tribofilm composition.[4,5] In addition, the decomposition reactions are often dictated by the true local conditions of temperature, pressure and shear at the asperity contacts rather than the calculated and imposed ones.[6] This complicates and obscures the correlations between the operational conditions and the decomposition kinetics of the ZDDP.

In spite of these hurdles, there is a solid consensus that under rubbing and heating, the ZDDP decomposes to form a protective tribofilm that consists mainly of Zn, P, S and O. This was confirmed using various surface analysis techniques including Scanning Electron Microscopy (SEM),[7,8]

X-ray Photoelectron Spectroscopy (XPS)[9,10] and X-ray Absorption Near Edge Spectroscopy (XANES).[11,12] The majority of these studies were performed ex-situ mainly on mature tribofilms, i.e. after formed on rubbed surfaces for a long time. Fewer other studies used in-situ techniques such as XANES,[11,13,14] XPS,[15,16] Raman spectroscopy[17,18] and Attenuated Total Reflectance (ATR)-FTIR.[19,20] However, most of these in-situ techniques suffer from various limitations including the need for high vacuum environment, special coated substrates or limited operating conditions of temperature and load. There are other few studies[12,21,22] that have attempted to examine the decomposition process and the change in the tribofilm composition primarily during the running-in period. This period occurs in the beginning of the tribological test at short rubbing times ranging from few minutes to a couple of hours depending on the type of lubricant and severity of the operating conditions. During this period surface smearing and wear can occur due to the asperity interactions, which can change the surface roughness, lubrication regime and consequently friction. After the running in period, friction typically reaches steady-state value. The lack of extensive studies focusing on the early stage of the reaction makes it difficult to gain insight into the exact reaction pathways of the ZDDP decomposition and its associated kinetics. For instance, it is still unclear why the short chain phosphates are present in the bulk of the tribofilm near the metal surface as opposed to the long ones near the tribofilm surface. Fuller et al.[23] related this to the reaction between the long chain phosphate and water, which can depolymerize the

*Corresponding author:
Abdel Dorgham (a.dorgham@leeds.ac.uk)

long chains into shorter ones. Others[24] related it to the ability of phosphate glass to dissolve sulfides. Furthermore, several other studies[21,25–27] suggested that the cation exchange reaction between Fe and Zn necessitates the depolymerization of the long chains, which ends up forming a composite Fe-Zn polyphosphate matrix of short chains. However, this reaction requires temperatures as high as 1300 K,[28] which are not attainable during any normal tribological conditions. Nonetheless, it was suggested that the local temperature, i.e. the flash temperature, at the asperity-asperity contacts can be much higher than the oil temperature when rubbing under high contact pressures and hence the reaction can occur even when the lubricant itself is at ambient temperature.[28] The evidence for the formation of the Fe-Zn polyphosphate was drawn based on the observation that iron is present in the tribofilm and its concentration increases towards the metal surface.[1,21,29] This observation was mainly based on sputtering the tribofilm with an ion gun to acquire spectra at different depths, i.e. depth profiling. However, depth profiling can induce preferential sputtering, i.e. better yield, of certain components of the tribofilm more than the others, which can be misleading.[30] Therefore, the results from sputtering experiments should be complemented with other methods such as Focused Ion Beam (FIB) for cross sectional analysis of the samples using Transmission Electron Microscope (TEM) coupled with Energy-dispersive X-ray (EDX) spectroscopy.

In contrast to the studies based on sputtering, other studies[12,22] showed that iron is absent in the formed tribofilm. In particular, Nicholls et al.[12] showed that even after 10 s of rubbing the phosphate has most likely Zn^{2+} cations rather than Fe^{2+}.

Another unclear matter is related to the exact pathways of the ZDDP decomposition reactions and their associated kinetics. Yin et al.[21] proposed a mechanism for ZDDP tribofilm growth starting with the strong chemisorption of ZDDP to the oxide layer on the metal surface. This is followed by the fast formation of long polyphosphate chains and the slow formation of short phosphate chains. On the other hand, Jones and Coy[31] proposed that the decomposition of ZDDP starts with the migration of the alkyl groups from oxygen to sulfur atoms, i.e. by self-alkylation or transalkylation, followed by the formation of phosphoric acid as a result of thioalkyl (−SR) elimination. Finally, the phosphate chains P−O−P are formed as a result of nucleophilic substitution of one phosphorus species with another. To validate the occurrence of these reactions, evidence based on surface analysis techniques, e.g. XPS and EDX, was presented to support the identification of the different species formed during the ZDDP decomposition. Nevertheless, no information has been provided on the rate of formation of these species as a function of time under constant temperature and contact pressure. Therefore, this study aims at examining the decomposition process of ZDDP over different rubbing times especially during the early stages of the reaction. This should give more insight into not only the reaction kinetics but also the composition of the formed triboreactive film.

Experimental

Lubricants

The lubricant used in this study was obtained from Afton Chemical, UK, which consists of a poly-α-olefin (PAO) synthetic oil containing secondary ZDDP antiwear additive (0.08% P) and a trace of ester to aid in solubility. The oil has a density of 830 kg.cm^{-3} and a viscosity of 45 cSt at 30 $^{\circ}$C and 4 cSt. at 100 $^{\circ}$C.

Tribological tests

The countersurfaces used to perform the tribological tests consist of a ball and disc made of AISI 52100 bearing steel. The ball, $D = 19$ mm, and disc, $D = 46$ mm, are polished and both have a nominal root mean square (RMS) roughness of better than 13 nm (Fig. S2). All the tribological tests were performed at a constant temperature of 80 $^{\circ}$C. The Mini-Traction Machine (MTM) rig shown in Fig. 1, was used to perform the tribological tests under rolling and sliding conditions due to its capability to rotate the ball and disc independently. The level of slide-to-roll ratio (SRR) was fixed at 5%, which is defined as the ratio of the speed difference between the two contacting surfaces to their average speed, i.e. the entrainment speed. This corresponds to mainly rolling conditions with a minuscule amount of sliding. The decomposition reaction and tribofilm formation cannot occur under pure rolling conditions but adding a small sliding percentage can induce such a reaction but at a slow rate. This provides a means to capture the early stage of the reaction and the formation of any intermediate species before the tribofilm formation. The average tribofilm thickness after different rubbing times, i.e. after 2.5 and 5 minutes and subsequently after every 10 minutes, was measured using the spacer-layer imaging method (SLIM) in the MTM rig.

The tribological tests using the MTM were carried out at an entrainment speed of 35 mm/s and a normal load of 60 N, which corresponds to a contact pressure of 1.2 GPa. The lubrication regime under these conditions was estimated using the Hershey number, which was found close to zero indicating boundary lubrication. The lubrication regime was also estimated by calculating the λ ratio, which represents the ratio of the minimum film thickness to the composite RMS surface roughness of the two contacting surfaces. This ratio was estimated to be 0.06, which suggests that the lubrication regime is boundary. However, this is only valid in the beginning of the tribological test because surface smearing and wear can occur during the running-in period due to the asperity interactions, which can change the surface roughness and hence the lubrication regime. Nevertheless, it was estimated

Fig. 1. Schematic of the mini-traction machine (MTM) used to perform all the tribological tests. It consists of a ball and disc, which can be rotated independently to achieve different slide-to-roll ratios.
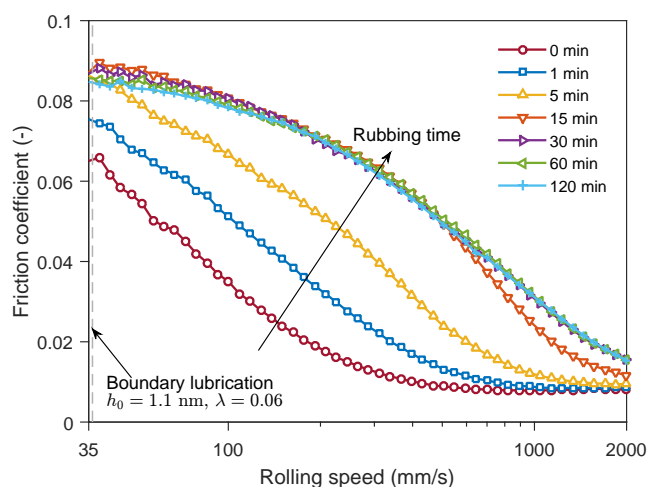
Fig. 2. Stribeck curves of the PAO-ZDDP oil after different rubbing times. The vertical dashed line indicates the speed of 35 mm/s at which all the tribological tests were performed.

that even if the surface roughness of the disc and ball drops from 13 nm to 3 nm, λ is still much below 1, i.e. 0.27, and hence the lubrication regime is still boundary. To validate this estimation, different Stribeck curves were obtained after different rubbing times as shown in Fig. 2. It is evident that for the chosen speed of 35 mm/s the lubrication regime remains boundary during the whole period of the tribological test, i.e. 120 minutes.

Surface analysis

XPS. The XPS analysis was performed using a PHI (Model 5000) Versa Probe spectrometer (ULVAC-PHI, Chanhassen, MN, USA). The X-ray source used to collect all the spectra is a monochromatic Al Kα (23.7 W, 1486.6 eV), which has a beam diameter of 100 μm. For Al Kα radiation, the sampling depth from which 95% of all photoelectrons are scattered without inelastic events is 3-10 nm. The source analyzer angle at which the photoelectrons were collected

was fixed at 45°. Using these configurations, the XPS measurements can be safely assumed to represent a good average of the relatively large probed volume without the complication of assuming a heterogeneous layered system. This is especially true considering that within the probed depth of the tribofilm, the composition changes gradually rather than abruptly. A survey scan and high resolution scans of six regions of interest, i.e. C1s, O1s, Fe2p, P2p, Zn2p and S2p, were acquired simultaneously for all the samples at four locations, i.e. three inside and one outside the wear scar. Zn3s signal was acquired within the same region of P2p. The survey scans were carried out in a fixed analyzer transmission (FAT) mode using a pass energy of 187.85 eV and an energy step size of 0.5 eV. The high resolution spectra were also acquired in FAT mode but using a pass energy of 46.95 eV and an energy step size of 0.05 eV. During the different signal acquisitions, the pressure of the main ultra-high vacuum chamber was below 1.0×10^{-7} Pa.

The analysis of the spectra was performed using CasaXPS software (v2.3.17). The background baseline of all the signals was subtracted using a standard Shirley background line type. As Fe2p, P2p, S2p and Zn2p have a spin-orbit splitting, which means that the total signal is formed of a doublet of 2p 3/2 and 2p 1/2, only the prominent signal of 2p 3/2 was reported in this study.

The deconvolution of the different components within all the signals was performed by fitting them with peaks having Gaussian/Lorentzian product formula line shape. The different parameters and constraints used for fitting the spectra and the assignments to these peaks were obtained based on the available literature of standard samples of similar composition to ZDDP tribofilm.[9,28,32,33] Although the fitting parameters especially the FWHM might change from one instrument to another, applying the same set of parameters to the whole dataset can still be used to analyze the rates of change but not the exact absolute values. The standard deviation of the positions of the XPS peaks was reported based on the mean across three repetitions. To compensate any charging during the data acquisition, the difference between the measured binding energy of the aliphatic component (C–C, C–H) of C1s signal and its expected value at 285.0 eV was used to shift the binding energy of the other signals. Furthermore, an additional calibration was performed, using the method proposed by Smith,[34] to account for the effect of the adventitious hydrocarbon contamination layer on the surface of the samples on the intensity of the signals of interest. The full analysis in provided in Fig. S1 and Tables S1 to S6.

FIB. A thin section across the wear scar (Fig. S3) was prepared using a precise high resolution FIB microscope (FEI Nova 200 NanoLab) equipped with a Field Emission Gun - SEM (FEG-SEM). The tilt of the sample was precisely controlled using an automated positioning stage fitted inside the FIB microscope. In order to minimise the tribofilm dam-

age, initially a Pt-based protection layer of a thickness about 70 nm was sputtered and deposited on the tribofilm using electron-beam induced deposition (EBID) using metal carbonyls of Me(CO)x as a precursor. The low energy electron impact typically does not result in any significant damage to the substrate, as indicated in the clean interface between the tribofilm and the EBID layer. However, it causes carbon contamination from the carbon-based precursor throughout the deposited layers. A second thick Pt layer of about 500 nm, which is sputtered using ion beam- induced deposition (IBID) through a 30 keV Ga$^+$ focused ion beam, was deposited on the initial layer. The high energy Ga$^+$ ions caused damage to the initially deposited sacrificial protection layer of Pt/C, which was manifested in the appearance of a third layer between the first base layer of Pt/C and the second top layer of Pt/Ga/C.

TEM/EDX. The prepared thin section was imaged using a 200 kV TEM (FEI Tecnai TF20), which is fitted with a high angle annular dark field (HAADF) detector. The composition across the prepared section was examined by acquiring EDX spectra at different points across the sample using Oxford Instruments INCA 350 EDX system with X-Max SDD detector fitted to the TEM. The EDX analysis including the quantification of the maps and spectra peaks was performed using AZtec software v2.1 (Oxford instruments, UK) for O, P, S, Zn, Fe and C elements while neglecting H, which cannot be detected by TEM-EDX. The TEM-EDX measurements were performed once and thus the analysis is only used to qualitatively follow the concentration evolution of the elements of interest but not to quantitatively measure absolute values.

Results

Tribological tests

The evolution of the friction coefficient and tribofilm thickness over 120 minutes of rubbing time is shown in Fig. 3. The friction coefficient evolves through three different stages. The first one, which occurs within the running-in period during the first 20 minutes, is characterized by a sharp increase in the friction coefficient from 0.058 to 0.09. On the other hand, the second stage, which occurs between 10 and 40 minutes, is characterized by a progressive decrease in the friction coefficient from 0.09 down to 0.075. Finally, in the last stage, the friction coefficient stays at a steady state value of about 0.076.

The overall behavior of the tribofilm thickness, which is shown on the same Fig. 3, resembles a similar trend to the one of the friction coefficient in terms of two general features. First, during the early stages of the tribological test in which friction increases, the tribofilm thickness is initially stagnant then grows. Second, after the running-in period as the friction coefficient reaches steady state, the tribofilm
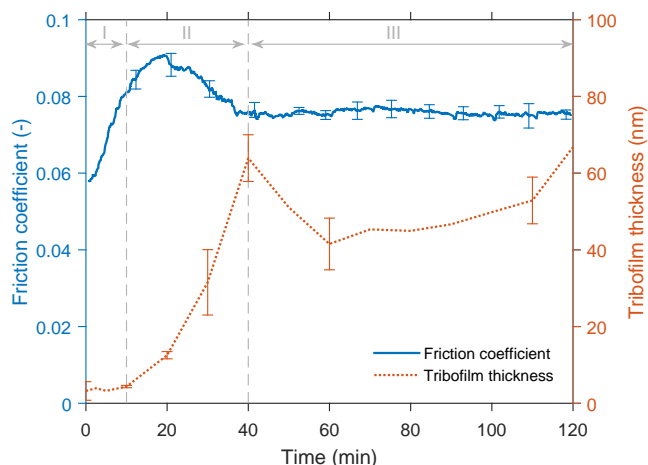
Fig. 3. Evolution of the friction coefficient and tribofilm thickness over different rubbing times. It consists of three stages: (I) rubbing-in, (II) tribofilm formation and (III) steady state.

thickness in general decreases and increases until reaching an average terminal value of about 70 nm after 120 minutes of rubbing. However, some differences were observed between the evolution of the friction coefficient and tribofilm thickness. For instance, during the early stage during which the friction coefficient grows steadily, the tribofilm thickness was initially stagnant, which then started to increase with a rate of 2.3 nm/min before decreasing to its peak value around 65 nm after 40 minutes. These different kinetics that govern the evolution of friction and tribofilm growth indicate that the changes in the friction coefficient are not only a function of the tribofilm thickness but possibly the composition as well, e.g. the length of the phosphate chains composing the main bulk of the tribofilm.

Wear is not reported in this work as it was insignificant in all the tribological tests. This indicates that even after 120 minutes of rubbing, the tribofilm was largely durable to the extent that it provided a full protection to the steel surface underneath.

Surface analysis

TEM/EDX cross-section analysis. To examine the changes in the composition of the ZDDP tribofilm over its depth, a postmortem cross section was prepared using FIB and analyzed using TEM/EDX. Fig. 4a shows a section across the tribofilm formed in the last stage of the tribotest after 120 min of rubbing. The tribofilm was found to have an average thickness of 75 ± 5 nm, which matches the one measured by MTM-SLIM and reported in Fig. 3. Furthermore, the tribofilm shows two distinctive features. The first one consists of small dark regions across the tribofilm (about 20 % of the tribofilm as shown in Fig. S4), which are mainly
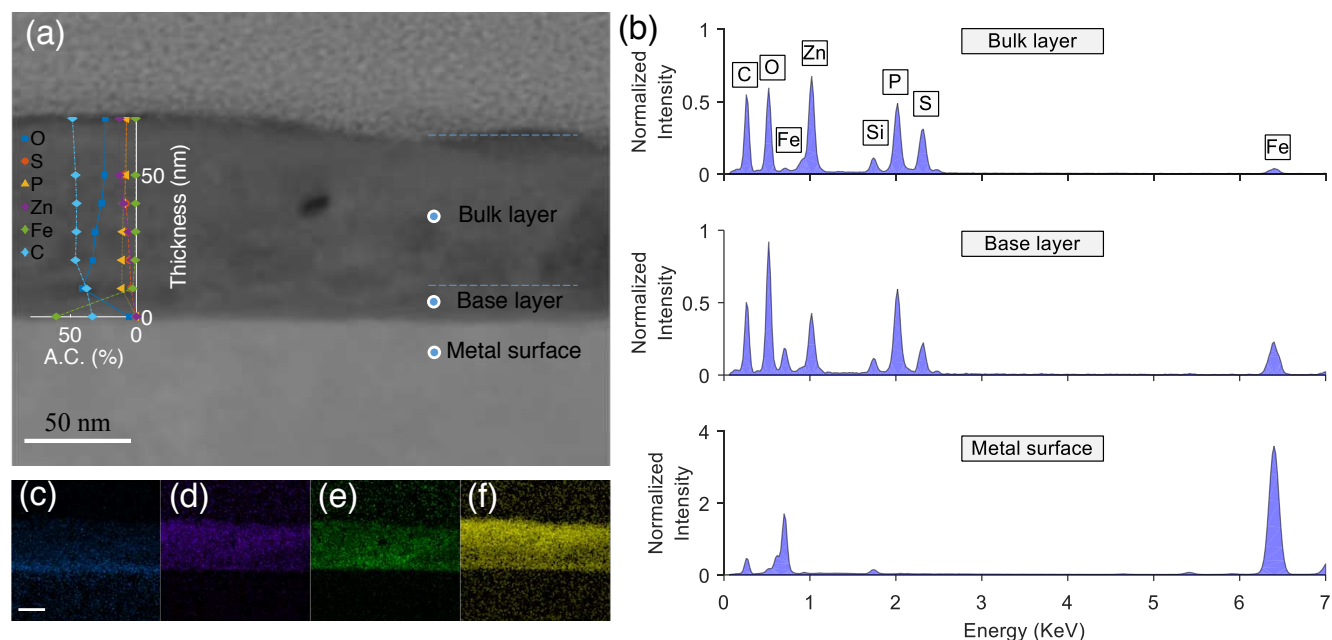
Fig. 4. TEM-EDX analysis, which includes (a) cross-section of the wear scar after 120 min of rubbing. EDX analysis is also shown for the atomic concentrations of the main tribofilm components, i.e. O, S, P and Zn. (b) EDX spectra of the three main regions, i.e. the steel surface and the bottom base and bulk layers of the tribofilm. (c)-(f) EDX maps of O, S, P and Zn, respectively, across the tribofilm shown in (a).

rich in carbon (Fig. S5). These dark regions were observed in multiple samples, which indicate that they represent a genuine part of the tribofilm. These regions can also be observed in previous publications by Ito and co-workers[35,36] where they used different contrast such that the dark regions in our case appear white in their TEM images. The origin of these regions can be speculated to be due a hastened formation phase during the decomposition of the ZDDP molecules and formation of the tribofilm.

The remaining majority of the tribofilm extends between the steel surface and the tribofilm's top layer. A comparison between the EDX spectra of the steel surface and the tribofilm's base and bulk layers is shown in Fig. 4b. The results indicate that the tribofilm consists mainly of P, O, S, Zn and Fe. The tribofilm also contains a small concentration of C (Fig. S6) and possibly H, which cannot be detected by TEM-EDX. From the base to the bulk layers of the tribofilm, the concentration of Fe decreases sharply (Table S7). This can possibly be due to two reasons. Firstly, as the thickness of the base layer is small, i.e. < 10 nm, a small misalignment of the cross-section can cause the EDX to pick a signal from the steel surface. Secondly, wear and mechanical mixing occurring near the steel surface can cause iron particles and cations to be digested in the tribofilm's layers. This is evident from the large concentration of oxide, sulfur and other elements in the base layer, as shown in the EDX maps in Fig. 4c-f.

The changes in the atomic concentrations of the main elements forming the tribofilm were calculated from several EDX spectra across the tribofilm and shown in the inset of Fig. 4a. The results show that the atomic concentrations of P, S and Zn in the layers starting from the base to the outer layer monotonically increase until reaching steady state value. In contrast, the concentration of oxygen monotonically decreases until reaching steady state. Another distinctive feature in the EDX results is the evolution of P and Zn. The results indicate that in the layers near the steel surface the concentration of P is slightly higher than the one of Zn. This trend reverses toward the surface of the tribofilm with the progressive increase in the concentration of Zn and nearly constant concentration of P.

XPS peaks identification. The different high resolution signals acquired from the different regions of interest, i.e. O1s, C1s, S2p, Fe2p, P2p, and Zn3s, on as-prepared discs (Fig. S7) and inside (Fig. 5) the wear scar were fitted with different peaks in order to identify the different components contributing to the total signal. The summary of this analysis is presented in Table 1.

The O1s signal was fitted with three peaks as shown in Fig. 5a,b, which were ascribed to the three main species of oxygen that the tribofilm is expected to have. The first one is the bridging oxygen (BO) identified at 533.1 ± 0.2 eV,[9,33,37] which represents the oxygen bridging the phosphorus atoms in the phosphate chains (P−O−P). The second one is the non-bridging oxygen (NBO) identified at 531.8 ± 0.2 eV,[9,37,38] which represents mainly the oxygen within a terminating phosphate group (−PO$_x$) such as −P=O, P−O−Zn and

Table 1

XPS component analysis of the binding energies and ratios of the different elements forming the ZDDP tribofilms after different rubbing times from 2.5 to 120 minutes. The green line in all the figures represents a standard Shirley background line type.

Time (min)	2.5	5	10	20	30	60	120
Component		Binding energy (± 0.05 eV)					
O1s: BO (eV)	533.05	532.25	533.09	532.76	533.06	533.13	533.15
O1s: NBO (eV)	532.79	531.92	531.82	531.21	531.73	531.70	531.72
O1s: MO (eV)	530.25	530.60	530.65	530.73	-	-	-
Zn3s (eV)	-	140.36	140.47	140.42	140.42	140.40	140.31
P2p 3/2 (eV)	133.55	133.57	133.64	133.64	133.53	133.64	133.66
S2p 3/2 (eV)	162.13	162.22	162.33	162.27	162.23	162.37	162.31
				Ratio			
BO/NBO	0.22	0.25	0.28	0.32	0.26	0.34	0.38
P/O	0.20	0.35	0.42	0.51	0.48	0.53	0.45
P/Zn	1.06	0.99	0.96	1.06	1.26	1.25	1.35
S/Zn	0.56	0.69	0.58	0.72	0.80	0.93	1.21

P−O−Fe(III)[39] as well as other species such as iron carbonate, oxy-hydroxide and sulfates. The contribution from these species in the first 20 minutes when the reaction layer is thin (Fig. 3) can be important, though might be alleviated at the high temperature tests due to evaporation, but it will only affect the BO/NBO ratio and O1s (BO+NBO) concentration. The third contribution to O1s signal is the metal oxide, e.g. FeO and Fe_2O_3, which was detected at 530.6 ± 0.2 eV[40] only during the running-in period, i.e. < 20 minutes.

The P2p 3/2 peak is shown in Fig. 5c,d. Initially, it appeared at 133.55 ± 0.1 eV, which can be assigned to zinc thiophosphate[41] or possibly $Fe(PO_4)$.[29] With the progression of rubbing, i.e. after 120 minutes, the binding energy shifted to 133.66 ± 0.1 eV, which indicates that the phosphate polymerizes to form long phosphate chains.[42]

Zn3s is also shown in Fig. 5c,d. It appeared at 140.4 ± 0.1 eV and did not exhibit any change between 2.5 minutes and 120 minutes of rubbing to within the energy resolution of the XPS measurements. This is in agreement with other studies, which found that the Zn3s signal does not change with composition but fixed at 141.0 ± 0.1 eV[42] or 140.0 ± 0.2 eV.[37] Similarly, the binding energy of Zn2p (Fig. S8) appeared at a fixed position at 1021.5 ± 0.1 eV. The species at these binding energies can be equally assigned to ZnS, $Zn(SO_4)$ and ZnO[32] or zinc phosphate.[28]

The S2p (II) 3/2 peak appeared at 162.2 ± 0.1 eV, as shown in Fig. 5e,f. This low binding energy can be assigned to sulfide[32,41] or equally to thiophosphate or organosulfur.[32] The uncertainty in the assignment is related to the inability of the XPS to resolve the metal sulfide from thiophosphate or similar thiols. No sulfate signal was detected after the different rubbing times except at the beginning of the test, i.e. after 2.5 minutes, which appeared at 168.6 ± 0.2 eV. This

sulfate can be assigned to $FeSO_4$ or $Fe_2(SO_4)_3$,[43] which corresponds to about 15% of the total amount of sulfur whereas the sulfide represents the remaining amount. The formation of sulfate species during the early stage of rubbing can be driven primarily by the local available temperature, i.e. the flash temperature at the asperities.[21] Below the critical temperature for this reaction to occur, the ZnS is expected to form instead.

The Fe2p 3/2 signal (Fig. S8) was detected only during the running-in period, i.e. rubbing times less than 30 minutes, which suggests that a mixture of FeO and Fe_2O_3 is present on the steel surface. Three main peaks were identified. The first one, which appeared at 709.0 ± 0.2 eV, can be assigned to Fe(II) oxide[33,41] and possibly FeS.[44] The second peak position was identified at 710.5 ± 0.2 eV, which can be assigned to Fe(III) oxides or $FeSO_4$.[41,45] The third peak was identified at 707.1 ± 0.1 eV during the first 2.5 minutes of rubbing, which can be assigned to metallic iron,[32,45] or FeS_2.[43] Additional two peaks appeared at high binding energies of 714.0 ± 0.2 eV and 718.8 ± 0.2 eV, which were assigned to Fe(II) and Fe(III) satellites,[46] respectively. A good correlation exists between the areas of the iron oxides in Fe2p 3/2 and the one of the metal oxides (MO) in O1s (Tables S2-S4). The ratio between Fe(II):Fe(III):O(MO) was close to 1:2:4, which indicates that the oxides exists as Fe_2O_3.

The C1s signal was mainly fitted with a single peak at 285.0 eV as shown in Fig. 5g,h, which was ascribed to aliphatic carbon (C-C, C-H). However, near the steel surface, i.e. after rubbing times < 10 minutes, two more peaks were identified at 286.5 ± 0.2 and 288.6 ± 0.2 eV. These peaks were assigned to hydroxyl (COH) and carboxyl (COOH) groups, respectively.[47]

Evolution of decomposition species. The atomic concentrations of the different elements composing the ZDDP tribofilm after various rubbing times measured by XPS are shown in Fig. 6 along with the ones obtained by the TEM-EDX analysis. The rubbing time for the points based on the EDX was obtained by matching the thickness at which the EDX point was measured with the one measured by MTM-SLIM after a certain rubbing time, which was reported in Fig. 3. A good agreement between the the two methods was found for the evolution trends of the measured concentrations but their absolute values. The two methods indicate that during the running-in period, i.e. < 20 minutes, the concentrations of Zn, P and S increased substantially whereas the concentration of O decreased abruptly. However, after the running-in period, these concentrations start to approach an equilibrium state with no further change.

Based on the XPS analysis, the evolution over rubbing time of the BO/NBO, P/O and P/Zn ratios is shown in Fig. 7 and summarized in Table 1 along with S/Zn. These ratios are important for two reasons. First, the P/O and BO/NBO ratios can be used as indications of the polymerisation number
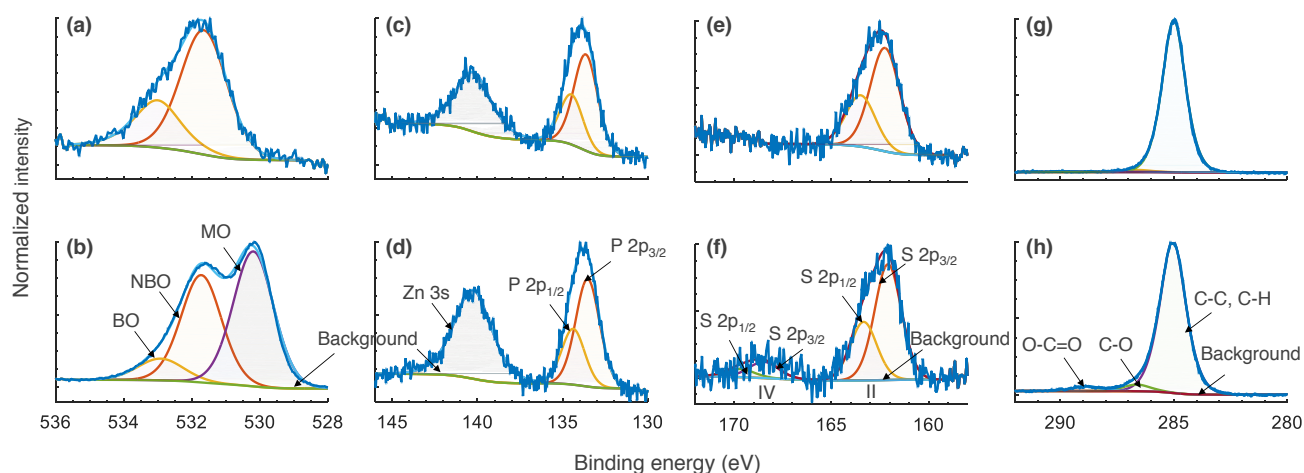
Fig. 5. Peak fitting analysis of the different components composing the XPS signals of (a,b) O1s, (c,d) P2p and Zn3s, (e,f) S2p and (g,h) C1s. The lower row is after 2.5 minutes of rubbing whereas the upper one is after 120 minutes.
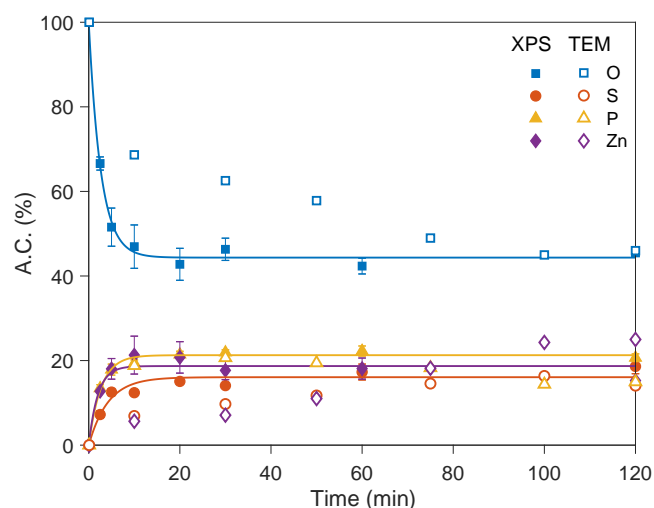
Fig. 6. Evolution of the atomic concentrations of the elements found in the ZDDP tribofilms after different rubbing times. Solid symbols are based on the XPS analysis and open symbols are based on the EDX analysis. Solid lines are the fits of the model described in Eq. (9).
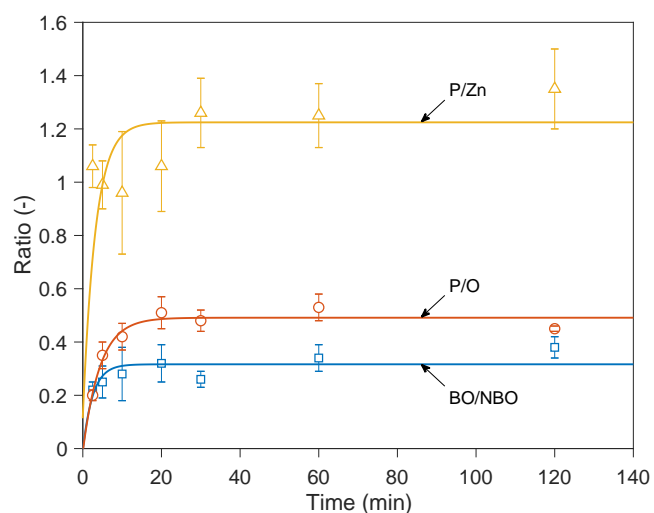
Fig. 7. Evolution of the BO/NBO, P/O and P/Zn ratios based on the XPS analysis of the ZDDP tribofilms after different rubbing times. Solid lines are the fits of the model described in Eq. (9).

of the zinc thiophosphate chains composing the main bulk of the ZDDP tribofilm. Thus, comparing these ratios would help follow the growth of the phosphate chains. The S/P and S/Zn ratios are not important if the tribofilm is viewed as consisting of zinc sulfide dissolved in a zinc phosphate matrix. However, they are important in case of viewing the tribofilm as consisting of zinc thiophosphate matrix. The XPS results indicate that for the immature tribofilms formed at the beginning of the tribotest, i.e. $\leq$ 5 minutes of rubbing, the BO/NBO, P/O, P/Zn and S/Zn ratios were low, i.e. 0.22, 0.20, 1.06 and 0.56, respectively. This suggests the initial

formation of short chain zinc thiophosphate, $Zn_3(PSO_3)_2$, as identified in the XPS stoichiometric analysis presented in Tables S5 and S6. The formation of short chain thiophosphate was also reported before by Heuberger et al.[41]

In the more mature tribofilms formed between 5 and 120 minutes of rubbing, the XPS analysis revealed a general increase in the ratios of BO/NBO, P/O, P/Zn and S/Zn over rubbing time, e.g. the P/O and S/Zn ratios were doubled whereas the P/Zn ratio increased by about 30%. The stoichiometric analysis of these ratios indicates that the initially formed short chains of zinc thiophosphate, $Zn_3(PSO_3)_2$, are polymerized into longer chains, $Zn_2P_2S_2O_5$.

Discussion

Tribofilm formation and friction

The initial transient changes in the friction coefficient shown in Fig. 3 can be related to different effects. First, surface smearing and wear can occur during the running-in period due to the asperity interactions, which can change the surface roughness. However, in this study wear was insignificant as the tests were performed using smooth countersurfaces under nearly rolling conditions. Second, changes in the effective surface roughness can occur due to the patchiness of the growing ZDDP tribofilm on the rubbing surfaces. Nonetheless, the results of Taylor and co-workers[48,49] showed that even smooth ZDDP tribofilms can increase the friction coefficient. This suggested that whether the ZDDP tribofilm is rough or smooth, it may inhibit the entrainment of the lubricating film between the rubbing contacts leading to higher friction. Furthermore, Taylor and Spikes[48] suggested that this apparent increase in friction could actually mean that the tribofilm is capable of maintaining the boundary lubrication condition for longer time than in the case of bare contacts without a tribofilm. These results indicate that the transient changes in the tribofilm thickness and friction coefficient shown in Fig. 3 can be intercorrelated. However, although the tribofilm thickness resembles a similar trend as the one of the friction, the timing is not exactly aligned, which is in line with the results of Taylor and Spikes.[48] This indicates that the relation between the friction coefficient and tribofilm thickness is not a simple function, e.g. thicker tribofilm does not imply higher friction coefficient. To resolve this issue, the changes in the tribofilm morphology should be examined more closely along with its thickness. For instance, during the first 20 minutes of rubbing there is only a slight change in the thickness of the ZDDP tribofilm, however, this period encompasses the main changes in the friction coefficient as well as the main changes in the concentrations of the decomposition components deposited on the contacting surfaces (Fig. 6). The XPS results indicate that the increased ratios of P/O, P/Zn and BO/NBO during the early stages of the tribological test are related to the increase in the average length of the phosphate chains composing the main bulk of the tribofilm. This suggests that the phosphate chains covering the contacting surfaces can interact with each other depending on the chain length[50] and number of chain ends that are capable of interpenetrating across the tribofilms covering the contacting surfaces.[51] Thus, the increased friction of the antiwear tribofilms over time can also be explained based on the observations of Mazuyer et al.[50] that after a certain threshold of contact time the layers covering the rubbing surfaces can interact and hence the mechanical properties, e.g. shear elastic modulus and interfacial shear strength, become a function of the contact time. In the case of the ZDDP tribofilm, this means that the longer the rubbing time lasts, the more the phosphate chains are formed and the stronger the interactions become. This can explain the observed apparent increase in the friction coefficient with the tribofilm thickness. In addition, there are a couple of other possibilities for the increased friction force: i) increasing the local adhesion, ii) decreasing the reduced elastic modulus, iii) increasing the contact area whether due to reducing the local elastic modulus or asperity adhesion, and iv) increasing the chain length covering the contacting surfaces can increase the local viscosity of the lubricant film and tribofilm in the contact zone. This is supported by the results of Bec et al.,[52] which suggested that the contact pressure can compact the loose layers of the ZDDP tribofilm and transfer them into a solid polyphosphate.

The drop in the friction coefficient after 20 minutes and its steadiness after 60 minutes of rubbing can be possibly related to the local arrangements of the long phosphate chains, which after reaching a certain threshold of length can form an ordered structure in the direction of shear. This behavior is similar to the one of adsorbed layers of hydrocarbon molecules of cis 1-4 poly- isoprene in 2,4, dicyclohexyl-2-methylpentane[53] and of self-assembled monolayers such as alkanethiols and alkylsilanes,[54,55] alkylsilane[56] and alkoxyl.[57] It is worth noting that these structures are different from the one of the phosphate chains but the alignment of the chains in the direction of shear to reduce the interfacial shear stresses and thus friction can be similar.

Tribofilm composition

Induction period and base layer composition . The initial changes in the adsorbed ZDDP as revealed by XPS (Fig. 5) and XAS[11,58] surface analyses and MTM-SLIM (Fig. 3), which show that sulfur species are formed first without much growth in the tribofilm thickness followed by the formation of zinc thiophosphate species, suggest the presence of an initial induction period. This period can have great implications. It has been long suggested that the ZDDP decomposition reaction is multistage, which involves initially the elimination of the soft acid alkyl groups or their migration from the hard base oxygen atoms to the soft base sulfur atoms of thiophosphoryl.[59] This reaction was also proposed to be followed by the formation of intermediate species before the formation of a phosphorus-rich film on the metal surface.[1,31] Our results clearly support this hypothesis. The formation of zinc sulfide and sulfate species before the formation of the zinc thiophosphate-rich film indicates that these sulfur-based species are the main products of the intermediate reactions. These reactions involve primarily the sulfur atoms in the adsorbed ZDDP molecules on the metal surface. This is in agreement with different previous studies proposing that Fe/Zn sulfides[22,29,33,35] and Fe/Zn sulfates[29] can be present at the metal surface. The formation of these species can be a

result of the reaction of the adsorbed ZDDP with iron oxides or the hydroxyl (C-OH) and carboxyl (COOH) groups on the steel surface,[21] which were identified in the XPS C1s signal (Fig. 5) and confirmed by other researchers.[60]

The XPS (Fig. 5) and previously reported XAS[11,58] results indicate that initially sulfate and sulfides, linked to iron or zinc, are formed followed by the reduction of sulfate to sulfide. The XAS measurements of Dorgham et al.[11,58] were performed in-situ under helium atmosphere so the detected sulfate cannot be a result of any exposure to air or humidity. In addition, the observed reduction reaction cannot be a result of a growth of tribolayers covering the sulfate layers underneath as before 10 minutes of rubbing, the tribofilm thickness as measured by SLIM (Fig. 3) is barely growing, i.e. still < 5 nm, whereas this initial period encountered the major changes in the tribofilm composition. It should be noted that as all the Fe2p area is correlated with the area of metal oxides peak in the O1s signal, this suggests that no other iron species such as iron sulfide, sulfate or phosphate are formed. This indicates that the sulfur species are linked to zinc not iron. However, as iron fingerprint appeared in all XPS (Fig. 5) and TEM-EDX (Fig. 4) spectra of the layer near the steel surface but only in some of the XAS spectra, this suggests that the formed iron-based species most likely form patches rather than a continuous layer.

The formation of sulfide or sulfate species in the above reactions is predetermined by the competition between the oxidation and sulfidation processes.[61] In the beginning of the tribotest, oxidation dominates due to the abundance of oxygen in the oil and the easy access to the unprotected oxidized steel surface. This leads to the formation of sulfate species. However, as heating and rubbing continue, sulfidation dominates and forms sulfides only. The formation of sulfides and the reduction of sulfates to sulfides continue until a patchy oxide-sulfide mixed base layer is formed, which is in line with our XAS, TEM-EDX and XPS results discussed before. The formation of this layer was also reported by several previous studies.[27,62,63]

The formed patchy base layer of isolated clusters of mainly sulfides on the metal surface, as schematically depicted in Fig. 8, can play different vital roles in the decomposition of ZDDP and its adsorption to the surface. Firstly, owing to their higher hardness than the metal oxides,[62] they can form a barrier to protect the steel surface from adhesive wear. Secondly, the clusters can act as a bridge or a binder between the subsequent decomposition products, e.g. zinc thiophosphate, and the metal surface. Thirdly, the sulphur clusters can diffuse into the steel surface and thus initiating subsurface cracks. This mechanism can explain the increased rate of surface micropitting in rolling contacts lubricated with oils containing sulfur-based additives like ZDDP.[60] Evidence for this mechanism can be found based on the observations of Jahanmir[62] that no sulfur is present in the center of the pits
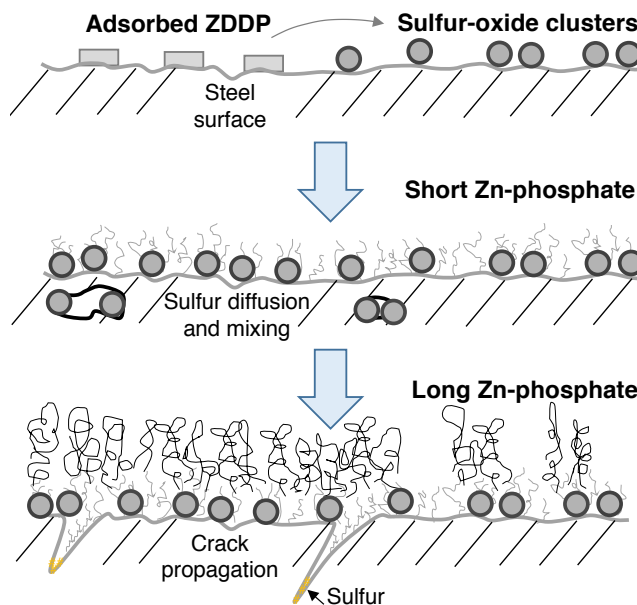
Fig. 8. Schematic of the formation of FeS clusters on the metal surface and the diffusion of S into steel, which induces stress corrosion cracking.

whereas Martin[27] found that sulfur is present in the wear particles. This indicates that delamination removed the center of the pit where sulfur is concentrated. The high concentration of sulfur in the center indicates that sulfur is concentrated in the tip of the subsurface crack where fatigue starts. This suggests that delamination can also be assisted by a possible diffusion of sulfur into the iron grain boundaries and thus promoting fatigue.

Bulk layers composition. The XPS results (Fig. 5) indicate that iron is absent from the formed zinc thiophosphate layers above the base layer, which agree with different previous studies.[12,22] The only cation observed was Zn, which was assigned to zinc thiophosphate, throughout the bulk layers. The absence of FeS away from near the metal surface is in agreement with the results of Zhang et al..[22] The authors observed the formation of both FeS and ZnS only in the beginning of the tribotest, i.e. after 10 s of rubbing, and ZnS only after longer rubbing times. They related this behavior to the more favorable reaction to form ZnS. This was also explained by Martin[27] on the basis of the hard and soft acids and bases (HSAB) principle and suggested that FeS can be formed only under severe conditions. On the other hand, our TEM-EDX results (Fig. 4) indicate the presence of a minuscule amount of iron in the bulk layers, which is much smaller in concentration than the one found in the base layer near the steel surface. The presence of iron along with zinc in the bulk layers can indicate the presence of mixed Fe-Zn tiophosphate. This is in agreement with some previous studies,[21,28,33] which proposed that a mixed Fe-Zn phos-

phate can form in the bulk. Nonetheless, Yin et al.[21] and later on Crobu et al.[28] have already indicated that the formation of these mixed phosphates of different cations requires much higher temperatures, i.e. above 1300 K, than the one of the oil, i.e. < 400 K, encountered during typical tribotests. Nonetheless, they suggested that the local flash temperature at the contacting sheared asperities can be higher and thus favors such a reaction. The maximum contact temperature T_c can be given using the following formula:

$$T_c = T_b + T_f \tag{1}$$

where T_b is the bulk temperature of the oil and T_f is the maximum flash temperature, which for circular contact with Peclet number of about 0.2 can be given as:[64]

$$T_f = 0.222 \frac{\mu U}{K} \left(p_y W \right)^{0.5} \tag{2}$$

where μ is the friction coefficient, U is the speed of the moving body in m/s, K is the thermal diffusivity in W/mK, p_y is the yield stress of the moving body in Pa, and W is the normal load in N. T_f can also be estimated using the simplified empirical model of Rabinowicz,[65] as follows:

$$T_f \approx 100U(1 \pm 3) \tag{3}$$

Under the operating conditions of our tests where the sliding and rolling speeds are small, the two previous models are expected to give similar results.[66] It was found that the flash temperature using Eq. (2) is about 4.5 ^{o}C, whereas using Eq. (3) is about 3.5 ± 10 ^{o}C. Using the upper estimated value of T_f = 13.5 ^{o}C, the contact temperature will be less than 93.5 ^{o}C. This suggests that it is likely that no mixed Fe-Zn phosphate can be formed at this low temperature. Nevertheless, it is worth mentioning that the nascent surface due to wear might promote such a reaction. This can be demonstrated based on the observation that the reaction of the nascent surface with sulfur is 1000 times faster than in the case of surface covered with oxide.[63] Furthermore, even if no mixed Fe-Zn phosphate are formed, the small Fe concentration detected by EDX but not XPS could mean than a small concentration of localized wear fragments is digested within the bulk layers. The digestion of such sharp wear particles is one of the known antiwear mechanisms of ZDDP to reduce abrasive wear.[27,67] This is further supported by the TEM-EDX results of Ito et al.,[35] which similar to our results show that iron is mainly present near the metal surface and its concentration declines sharply just above the base layer where the main bulk of the tribofilm consisting of zinc phosphate glass exists.

The XPS results indicate that initially short chains of zinc thiophosphate are formed followed by longer chains, which is evident from the evolution of BO/NBO, P/O and P/Zn ratios (Table 1 and Fig. 7). After a few minutes of rubbing, the average ratio of Zn:P:S:O was approximately 3:2:2:7, which suggests the formation of short chain phosphate of $Zn_3(PSO_3)_2$. Subsequently, after long rubbing time, i.e. > 20 min, the average ratio of Zn:P:S:O reached 2:2:2:5, which suggests the formation of medium chain phosphate of $Zn_2(PSO_2)_2O$. The polymerisation can originate from the nucleophilic reaction of one hard acid tetravalent phosphorus O−P in one short phosphate segment with a hard base oxygen bonded to another phosphate segment O−P, as follows:

$$\tag{4}$$
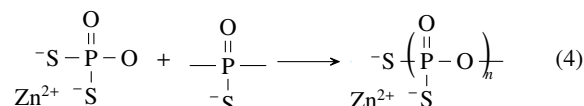
The formation of short chains in the base layer near the metal surface as compared to the long chains in the bulk is in agreement with several previous studies.[68–70] The trend can be related to the excess of metal oxides such as ZnO, FeO or Fe_2O_3, near the metal surface as compared to the bulk layers, which was verified experimentally using XPS (Figs. 5 and 6) and TEM-EDX (Fig. 4). Increasing the oxide content hastens the fragmentation of any formed long phosphate chains, i.e. P−O−P, into shorter chains of P−O$^-$ and P=O. Subsequently, the oxide can compensate the negatively charged fragments by forming weak electrostatic interactions with their terminals,[71] such as:

$$P{-}O{-}P + ZnO \longrightarrow P{-}O^- \cdots Zn^{2+} \cdots {}^-O{-}P \tag{5}$$

Other studies[41] attributed the reduced chain length near the metal surface to the shear stress between the contacting surfaces possibly cleaving the long phosphate chains into shorter ones and to severe surface wear that can remove the long phosphate chains from the surface. However, as our experiments were performed under nearly rolling conditions, i.e. 5% SRR, during which wear was insignificant, this indicates that other factors than the shear stress could play a role. Apart from ZnO, various studies[25,27,28] suggested that in the presence of iron oxide or water any formed long phosphate chains are depolymerized into short ones of Fe-Zn phosphates. This can explain the short phosphate chains and large concentration of iron detected in the base layer near the metal surface compared to the long phosphate chains and small iron concentration in the bulk layer.

Kinetics of ZDDP decomposition reaction

The tribofilm's main components, i.e. P, Zn, S and O, undergo two distinctive reaction phases over rubbing time, as indicated in the evolution of their atomic concentrations shown in Fig. 6. The first phase, which occurs during the running-in period, is characterized by a fast transient burst stage in which the atomic concentrations of the elements

forming the tribofilm grow exponentially despite the small increase in the tribofilm thickness. On the other hand, the second phase, which occurs at rubbing times > 20 minutes, is characterized by an intangible growth in the atomic concentrations that appear as asymptotically approaching steady state despite the fast growth in the tribofilm thickness over the same period. These two different phases indicate that the formation rate of the different species composing the tribofilm is not uniform throughout the tribological test. This observation is in agreement with the tribofilm thickness results discussed in Fig. 3 and the results of Gosvami et al.,[6] which suggested that during the early stage of rubbing, the tribofilm growth of ZDDP is slow and follows a linear trend but as rubbing continues the growth starts to exhibit a much faster logarithmic trend. Similar trend can also be seen in the results of Zhang and Spikes[72] for the ZDDP thermal film.

Gosvami et al.[6] suggested that the ZDDP additive decomposes initially with a zero reaction rate (n=0.12±0.11 using a free power law fit), which as rubbing continues increases to about 0.22±0.02. However, based on the observed growth trend of the ZDDP decomposition components, the first order kinetics model is more appropriate for the case of ZDDP as it has been reported before that the higher the initial concentration of ZDDP the longer the formed phosphate chains.[21] If the reaction is closer to zero order then increasing the concentration of the reactants should not have much influence on the products. This suggests that the polymerization reaction of the phosphate chains follows first-order reaction kinetics. Assuming that the polymerization of every chain starts with an initial concentration C_o of short chain phosphate and over time is polymerized into long polyphosphate chain with a concentration C_p, the following overall simplified reaction can be proposed:

$$C_o \xrightarrow{T,P,\dot{\gamma}} C_p \qquad (6)$$

As this is assumed to be a non-reversible reaction, the increase in the concentration of the formed chains over time can be expressed as:

$$\frac{d}{dt}\left(C_p\right) = k\left(C_o\right) \qquad (7)$$

where k is the reaction rate coefficient. To simplify the integration of this equation, C_o can be expressed in terms of the equilibrium concentration C_e at $t \rightarrow \infty$, as follows:

$$\frac{d}{dt}\left(C_p\right) = k\left(C_e - C_p\right) \qquad (8)$$

Upon integration and few arrangements, the solution to the above equation forms the first order rate law, which gives the concentration at any time t as:

$$C_p(t) = C_e\left[1 + \left(\frac{C_0 - C_e}{C_e}\right)\exp\left(-kt\right)\right] \qquad (9)$$

Table 2

Fitting parameters based on Eq.9 for the different components of the tribofilm.

Species	C_e (%)	C_0 (%)	k
O	44.35 ± 1.05	100	0.38 ± 0.07
P	21.27 ± 1.01	0	0.38 ± 0.09
Zn	18.70 ± 2.30	0	0.50 ± 0.33
S	16.07 ± 1.87	0	0.24 ± 0.12
BO/NBO	0.32 ± 0.06	0	0.40 ± 0.21
P/O	0.49 ± 0.04	0	0.23 ± 0.13
P/Zn	1.23 ± 0.20	0	0.31 ± 0.30

The model described in Eq. (9) is suitable in the case of a single growth or a single degradation of a component. However, in the case of phosphate chains in a tribofilm, they are expected to have a multimode mechanism of growth and cessation accompanied by a dynamic formation and removal of layers of the tribofilm. To account for this more complicated system, a model with two reaction rates can be used by adding the outcome of two models similar to the one described earlier in Eq. (9). The first model accounts for the growth whereas the second one accounts for the cessation or removal of the phosphate chains. In this case, the two are assumed to occur simultaneously and are mutually exclusive and hence the addition can be used. However, in the more complex tribological contact a strong synergy is more plausible as the longer the phosphate chains are formed the more the cessation or removal is expected. Nevertheless, for simplicity, the growth and cessation will be assumed to occur independently and non-contemporarily, and thus the single mode model described in Eq. (9) will be used to fit the data.

As the concentration of the short phosphate chains cannot be measured directly, the initial concentration of oxygen species will be used as an indirect indication of the concentration of the short chains. The argument is that initially an oxide layer covers the steel substrate. As the ZDDP molecules decompose, layers of short chains are formed (C_0 = 100 %). Then longer chains start to cover these layers gradually. So, as the polymerisation reaction evolves, the concentration of short chains (the reactant) decreases, whereas the concentration of the long chains (the product) increases. Thus, the evolution of O can be utilized to represent the evolution of short chains, whereas P, S and Zn species can represent the evolution of the chains in terms of their length. Using the fitting parameters listed in Table 2, Fig. 6 shows the results of fitting the proposed growth model to the XPS data of O, P, S and Zn, whereas Fig. 7 shows the fitting results for BO/NBO, P/O and P/Zn. The model fits the data extremely well using two fitting parameters only, i.e. C_e and k. The use of only two fitting parameters was justified by considering that initially no P, Zn or S exists on the surface, i.e. their

initial concentration $C_0 = 0$, but only O exits initially with $C_0 = 100$.

The fitting shows that the reaction rate coefficients k for the main components forming the phosphate chains, i.e. O and P, are similar, i.e. $k = 0.38 \pm 0.10$, which fall within the same range of the ones of BP/NBO, P/O and P/Zn ratios. The reaction rate of S is slightly lower, i.e. $k = 0.24 \pm 0.12$, whereas the one of Zn is relatively higher, i.e. $k = 0.50 \pm 0.33$. The difference in the reaction rates between the tribofilm's components might be a result of the larger deviation within the S and Zn data as indicated by the higher standard deviations of the model fitting coefficients.

Conclusion

This study followed the ZDDP decomposition reaction and its tribofilm formation over rubbing time. The study showed that before the formation of a phosphates-rich protective tribofilm, the ZDDP decomposition has an important precursor, namely, the formation of a sulfur-rich layer. The results suggest the necessity to form this base layer on the steel surface before any growth is possible. Hence, one can switch on and off the decomposition process by controlling the surface availability rather than the physical and chemical nature of the medium and surface. The sulfur precursors are formed nearly instantly, however the formation of the zinc thiophosphate has a transient burst phase near the steel surface followed by a slow phase until asymptotically approaching steady state. The formation of the zinc thiophosphate starts initially with short phosphate chains, which are formed due to the excess concentration of metal oxides on the steel surface. As the concentration of the oxides decreases away from the surface, this leads to the polymerization of the short chains into longer ones. Based on the observed growth trend of the ZDDP decomposition components, the polymerization reaction of the phosphate chains was suggested to follow first-order kinetics.

The findings of this study provide better understanding and new insights into the decomposition reactions and associated kinetics of the widely used ZDDP antiwear additive. The ZDDP reaction mechanisms revealed by this study can help make progress towards developing new green alternatives with similar antiwear capabilities.

Associated content

Supporting Information

Detailed calculations of the minimum film thickness, Hershey number and quantitative XPS stoichiometric analysis. Disc roughness by white light interferometry, TEM lamella, TEM-EDX and XPS spectra.

Author information

Corresponding author

*E-mail: a.dorgham@leeds.ac.uk

ORCID

Abdel Dorgham: 0000-0001-9119-5111

Notes

The authors declare no competing financial interest.

References

(1) Spikes, H. The History and Mechanisms of ZDDP. *Tribology Letters* **2004**, *17*, 469–489.

(2) Nicholls, M. a.; Do, T.; Norton, P. R.; Kasrai, M.; Bancroft, G. Review of the Lubrication of Metallic Surfaces by Zinc Dialkyl-Dithiophosphates. *Tribology International* **2005**, *38*, 15–39.

(3) Barnes, A. M.; Bartle, K. D.; Thibon, V. R. A Review of Zinc Dialkyldithiophosphates (ZDDPs): Characterisation and Role in the Lubricating Oil. *Tribology International* **2001**, *34*, 389–395.

(4) Yin, Z.; Kasrai, M.; Bancroft, G.; Fyfe, K.; Colaianni, M.; Tan, K. Application of Soft X-ray Absorption Spectroscopy in Chemical Characterization of Antiwear Films Generated by ZDDP Part II: the Effect of Detergents and Dispersants. *Wear* **1997**, *202*, 192 – 201.

(5) Parsaeian, P.; Van Eijk, M. C.; Nedelcu, I.; Neville, A.; Morina, A. Study of the Interfacial Mechanism of ZDDP Tribofilm in Humid Environment and its Effect on Tribochemical Wear; Part I: Experimental. *Tribology International* **2017**, *107*, 135–143.

(6) Gosvami, N.; Bares, J.; Mangolini, F; Konicek, A.; Yablon, D.; Carpick, R. Mechanisms of Antiwear Tribofilm Growth Revealed In Situ by Single-Asperity Sliding Contacts. *Science* **2015**, *348*, 102–106.

(7) Vengudusamy, B.; Green, J. H.; Lamb, G. D.; Spikes, H. A. Tribological Properties of Tribofilms Formed from ZDDP in DLC/DLC and DLC/Steel Contacts. *Tribology International* **2011**, *44*, 165–174.

(8) Aktary, M.; McDermott, M.; McAlpine, G. Morphology and Nanomechanical Properties of ZDDP Antiwear Films as a Function of Tribological Contact Time. *Tribology letters* **2002**, *12*, 155–162.

(9) Crobu, M.; Rossi, A.; Mangolini, F.; Spencer, N. D. Chain-Length-Identification Strategy in Zinc Polyphosphate Glasses by Means of XPS and ToF-SIMS. *Analytical and bioanalytical chemistry* **2012**, *403*, 1415–1432.

(10) Ye, J.; Araki, S.; Kano, M.; Yasuda, Y. Nanometer-scale Mechanical/Structural Properties of Molybdenum Dithiocarbamate and Zinc Dialkylsithiophosphate Tribofilms and Friction Reduction Mechanism. *Japanese Journal of Applied Physics* **2005**, *44*, 5358–5361.

(11) Dorgham, A.; Neville, A.; Ignatyev, K.; Mosselmans, F.; Morina, A. An In Situ Synchrotron XAS Methodology for Surface Analysis Under High Temperature, Pressure, And Shear. *Review of Scientific Instruments* **2017**, *88*, 015101.

(12) Nicholls, M; Najman, M.; Zhang, Z; Kasrai, M; Norton, P.; Gilbert, P. The Contribution of XANES Spectroscopy to Tribology. *Canadian journal of chemistry* **2007**, *85*, 816–830.

(13) Morina, A.; Zhao, H.; Mosselmans, J. F. W. In-situ Reflection-XANES Study of ZDDP and MoDTC Lubricant Films Formed on Steel and Diamond Like Carbon (DLC) Surfaces. *Applied Surface Science* **2014**, *297*, 167–175.

(14) Ferrari, E.; Roberts, K.; Sansone, M; Adams, D A multi-Edge X-ray Absorption Spectroscopy Study of the Reactivity of Zinc Di-Alkyl-Di-Thiophosphates Anti-Wear Additives: 2. In Situ Studies of Steel/Oil Interfaces. *Wear* **1999**, *236*, 259–275.

(15) Donnet, C; Martin, J.; Fontaine, J; Sánchez-López, J.; Quirós, C; Elizalde, E; Sanz, J.; Rojas, T.; Fernández, A The Role of CN Chemical Bonding on the Tribological Behaviour of CN$_x$ Coatings. *Surface and Coatings Technology* **1999**, *120*, 594–600.

(16) Donnet, C; Fontaine, J; Grill, A; Le Mogne, T The Role of Hydrogen on the Friction Mechanism of Diamond-Like Carbon Films. *Tribology Letters* **2001**, *9*, 137–142.

(17) Gauvin, M.; Dassenoy, F.; Minfray, C.; Martin, J. M.; Montagnac, G.; Reynard, B. Zinc Phosphate Chain Length Study Under High Hydrostatic Pressure by Raman Spectroscopy. *Journal of Applied Physics* **2007**, *101*, 063505.

(18) Berkani, S; Dassenoy, F; Minfray, C; Belin, M; Vacher, B; Martin, J.; Cardon, H; Montagnac, G; Reynard, B Model Formation of ZDDP Tribofilm from a Mixture of Zinc Metaphosphate and Goethite. *Tribology International* **2014**, *79*, 197–203.

(19) Piras, F. M.; Rossi, A.; Spencer, N. D. Combined In Situ (ATR FT-IR) and Ex Situ (XPS) Study of the ZnDTP-Iron Surface Interaction. *Tribology Letters* **2003**, *15*, 181–191.

(20) Rossi, A; Eglin, M; Piras, F.; Matsumoto, K; Spencer, N. Surface Analytical Studies of Surface-Additive Interactions, by Means of In Situ and Combinatorial Approaches. *Wear* **2004**, *256*, 578–584.

(21) Yin, Z.; Kasrai, M.; Fuller, M.; Bancroft, G. M.; Fyfe, K.; Tan, K. H. Application of Soft X-Ray Absorption Spectroscopy in Chemical Characterization of Antiwear Films Generated by ZDDP Part I: the Effects of Physical Parameters. *Wear* **1997**, *202*, 172–191.

(22) Zhang, Z; Yamaguchi, E.; Kasrai, M; Bancroft, G.; Liu, X; Fleet, M. Tribofilms Generated from ZDDP and DDP on Steel Surfaces: Part 2, Chemistry. *Tribology Letters* **2005**, *19*, 221–229.

(23) Fuller, M. L. S.; Kasrai, M.; Bancroft, G. M.; Fyfe, K.; Tan, K. H. Solution Decomposition of Zinc Dialkyl Dithiophosphate and its Effect on Antiwear and Thermal Film Formation Studied by X-ray Absorption Spectroscopy. *Tribology international* **1998**, *31*, 627–644.

(24) Weyl, W. A. Phosphate Glasses. *Chemical & Engineering News Archive* **1949**, *27*, 1048–1049.

(25) Martin, J. M.; Grossiord, C.; Le Mogne, T.; Bec, S.; Tonck, A. The Two-Layer Structure of ZnDTP Tribofilms: Part I: AES, XPS and XANES Analyses. *Tribology international* **2001**, *34*, 523–530.

(26) Pawlak, Z.; Kosse, V.; Oloyede, A.; Rauckyte, T.; Kopkowski, A.; Hargreaves, D. J.; Pai, R. B.; Macintosh, D. The Antiwear Effectiveness of Micellar Zinc Phosphates and Copper Oxide Through Friction-Induced Cross-Linking. **2006**.

(27) Martin, J. M. Antiwear Mechanisms of Zinc Dithiophosphate: a Chemical Hardness Approach. *Tribology letters* **1999**, *6*, 1–8.

(28) Crobu, M.; Rossi, A.; Mangolini, F.; Spencer, N. D. Tribochemistry of Bulk Zinc Metaphosphate Glasses. *Tribology letters* **2010**, *39*, 121–134.

(29) Mourhatch, R.; Aswath, P. B. Tribological Behavior and Nature of Tribofilms Generated from Fluorinated ZDDP in Comparison to ZDDP under Extreme Pressure Conditions–Part 1: Structure and Chemistry of Tribofilms. *Tribology International* **2011**, *44*, 187–200.

(30) Hofmann, S Sputter Depth Profile Analysis of Interfaces. *Reports on Progress in Physics* **1998**, *61*, 827.

(31) Jones, R.; Coy, R. The Chemistry of the Thermal Degradation of Zinc Dialkyldithiophosphate Additives. *ASLE Transactions* **1981**, *24*, 91–97.

(32) Eglin, M.; Rossi, A.; Spencer, N. D. X-ray Photoelectron Spectroscopy Analysis of Tribostressed Samples in the Presence of ZnDTP: a Combinatorial Approach. *Tribology Letters* **2003**, *15*, 199–209.

(33) Heuberger, R.; Rossi, A.; Spencer, N. D. XPS Study of the Influence of Temperature on ZnDTP Tribofilm Composition. *Tribology Letters* **2007**, *25*, 185–196.

(34) Smith, G. C. Evaluation of a Simple Correction for the Hydrocarbon Contamination Layer in Quantitative Surface Analysis by XPS. *Journal of electron spectroscopy and related phenomena* **2005**, *148*, 21–28.

(35) Ito, K.; Martin, J.-M.; Minfray, C.; Kato, K. Low-Friction Tribofilm Formed by the Reaction of ZDDP on Iron Oxide. *Tribology international* **2006**, *39*, 1538–1544.

(36) Ito, K; Martin, J.; Minfray, C; Kato, K Formation Mechanism of a Low Friction ZDDP Tribofilm on Iron Oxide. *Tribology transactions* **2007**, *50*, 211–216.

(37) Liu, E.; Kouame, S. D. An XPS Study on the Composition of Zinc Dialkyl Dithiophosphate Tribofilms and Their Effect on Camshaft Lobe Wear. *Tribology Transactions* **2014**, *57*, 18–27.

(38) Flambard, A.; Videau, J.-J.; Delevoye, L.; Cardinal, T.; Labrugère, C.; Rivero, C.; Couzi, M.; Montagne, L. Structure and Nonlinear Optical Properties of Sodium–Niobium Phosphate Glasses. *Journal of Non-Crystalline Solids* **2008**, *354*, 3540–3547.

(39) Minfray, C; Martin, J.; Esnouf, C.; Le Mogne, T; Kersting, R; Hagenhoff, B A multi-Technique Approach of Tribofilm Characterisation. *Thin Solid Films* **2004**, *447*, 272–277.

(40) Minfray, C; Martin, J.; De Barros, M.; Le Mogne, T; Kersting, R; Hagenhoff, B Chemistry of ZDDP Tribofilm by ToF-SIMS. *Tribology Letters* **2004**, *17*, 351–357.

(41) Heuberger, R.; Rossi, A.; Spencer, N. D. Pressure Dependence of ZnDTP Tribochemical Film Formation: a Combinatorial Approach. *Tribology Letters* **2007**, *28*, 209–222.

(42) Crobu, M.; Rossi, A.; Spencer, N. D. Effect of Chain-Length and Countersurface on the Tribochemistry of Bulk Zinc Polyphosphate Glasses. *Tribology Letters* **2012**, *48*, 393–406.

(43) Konno, H.; Sasaki, K.; Tsunekawa, M.; Takamori, T.; Furuichi, R. X-ray Photoelectron Spectroscopic Analysis of Surface Products on Pyrite Formed by Bacterial Leaching. *Bunseki Kagaku* **1991**, *40*, 609–616.

(44) De Donato, P.; Mustin, C; Benoit, R.; Erre, R. Spatial Distribution of Iron and Sulphur Species on the Surface of Pyrite. *Applied Surface Science* **1993**, *68*, 81–93.

(45) Descostes, M; Mercier, F; Thromat, N; Beaucaire, C; Gautier-Soyer, M Use of XPS in the Determination of Chemical Environment and Oxidation State of Iron and Sulfur Samples: Constitution of a Data Basis in Binding Energies for Fe and S Reference Compounds and Applications to the Evidence of Surface Species of an Oxidized Pyrite in a Carbonate Medium. *Applied Surface Science* **2000**, *165*, 288–302.

(46) Bhargava, G; Gouzman, I; Chun, C.; Ramanarayanan, T.; Bernasek, S. Characterization of the "Native" Surface Thin Film on Pure Polycrystalline Iron: A High Resolution XPS and TEM Study. *Applied Surface Science* **2007**, *253*, 4322–4329.

(47) Guan, X.-h.; Chen, G.-h.; Shang, C. ATR-FTIR and XPS Study on the Structure of Complexes Formed upon the Adsorption of Simple Organic Acids on Aluminum Hydroxide. *Journal of Environmental Sciences* **2007**, *19*, 438–443.

(48) Taylor, L. J.; Spikes, H. A. Friction-Enhancing Properties of ZDDP Antiwear Additive: Part I–Friction and Morphology of ZDDP Reaction Films. *Tribology Transactions* **2003**, *46*, 303–309.

(49) Taylor, L. J.; Spikes, H. A. Friction-Enhancing Properties of ZDDP Antiwear Additive: part II– Influence of ZDDP Reaction Films on EHD Lubrication. *Tribology transactions* **2003**, *46*, 310–314.

(50) Mazuyer, D; Tonck, A; Bec, S; Loubet, J.; Georges, J. Nanoscale Surface Rheology in Tribology. *Tribology Series* **2001**, 273–282.

(51) Chen, N.; Maeda, N.; Tirrell, M.; Israelachvili, J. Adhesion and Friction of Polymer Surfaces: the Effect of Chain Ends. *Macromolecules* **2005**, *38*, 3491–3503.

(52) Bec, S.; Tonck, A.; Georges, J.-M.; Coy, R.; Bell, J.; Roper, G. In *Proceedings of the Royal Society of London A: Mathematical, Physical and Engineering Sciences*, 1999; Vol. 455, pp 4181–4203.

(53) Georges, J.-M.; Tonck, A.; Loubet, J.-L.; Mazuyer, D.; Georges, E.; Sidoroff, F. Rheology and Friction of Compressed Polymer Layers Adsorbed on Solid Surfaces. *Journal de Physique II* **1996**, *6*, 57–76.

(54) Lio, A; Charych, D.; Salmeron, M Comparative Atomic Force Microscopy Study of the chain Length Dependence of Frictional Properties of Alkanethiols on Gold and Alkylsilanes on Mica. *The Journal of Physical Chemistry B* **1997**, *101*, 3800–3805.

(55) Kim, H. I.; Boiadjiev, V; Houston, J. E.; Zhu, X.-Y.; Kiely, J. Tribological Properties of Self-Assembled Monolayers on Au, SiOx and Si Surfaces. *Tribology Letters* **2001**, *10*, 97–101.

(56) Xiao, X.; Hu, J.; Charych, D. H.; Salmeron, M. Chain Length Dependence of the Frictional Properties of Alkylsilane Molecules Self-Assembled on Mica Studied by Atomic Force Microscopy. *Langmuir* **1996**, *12*, 235–237.

(57) Major, R. C.; Kim, H.; Houston, J.; Zhu, X.-Y. Tribological Properties of Alkoxyl Monolayers on Oxide Terminated Silicon. *Tribology Letters* **2003**, *14*, 237–244.

(58) Dorgham, A.; Parsaeian, P.; Neville, A.; Ignatyev, K.; Mosselmans, F.; Masuko, M.; Morina, A. In Situ Synchrotron XAS Study of the Decomposition Kinetics of ZDDP Triboreactive Interfaces. *RSC Advances* **2018**, *8*, 34168–34181.

(59) Mosey, N. J.; Woo, T. K. A Quantum Chemical Study of the Unimolecular Decomposition Mechanisms of Zinc Dialkyldithiophosphate Antiwear Additives. *The Journal of Physical Chemistry A* **2004**, *108*, 6001–6016.

(60) Nedelcu, I; Piras, E; Rossi, A; Pasaribu, H. XPS Analysis on the Influence of Water on the Evolution of Zinc Dialkyldithiophosphate–Derived Reaction Layer in Lubricated Rolling Contacts. *Surface and Interface Analysis* **2012**, *44*, 1219–1224.

(61) Batchelor, A.; Stachowiak, G. Some Kinetic Aspects of Extreme Pressure Lubrication. *Wear* **1986**, *108*, 185–199.

(62) Jahanmir, S. Wear Reduction and Surface Layer Formation by a ZDDP Additive. *Journal of tribology* **1987**, *109*, 577–586.

(63) Batchelor, A.; Cameron, A; Okabe, H An Apparatus to Investigate Sulfur Reactions on Nascent Steel Surfaces. *ASLE Transactions* **1985**, *28*, 467–474.

(64) Stachowiak, G.; Batchelor, A. W., *Engineering tribology*; Butterworth-Heinemann: 2013.

(65) Rabinowicz, E., *Friction and Wear of Materials*; Wiley, New York: 1965.

(66) Blau, P., *Friction Science and Technology: From Concepts to Applications, Second Edition*; Mechanical Engineering; CRC Press: 2008.

(67) Martin, J.; Grossiord, C.; Mogne, T. L. The Two-Layer Structure of ZnDTP Tribofilms: Part I: AES, XPS and XANES Analyses. *Tribology International* **2001**, *34*, 523–530.

(68) Wiench, J.; Pruski, M; Tischendorf, B; Otaigbe, J.; Sales, B. Structural Studies of Zinc Polyphosphate Glasses by Nuclear Magnetic Resonance. *Journal of Non-Crystalline Solids* **2000**, *263*, 101–110.

(69) Tischendorf, B; Otaigbe, J.; Wiench, J.; Pruski, M; Sales, B. A Study of Short and Intermediate Range Order in Zinc Phosphate Glasses. *Journal of non-crystalline solids* **2001**, *282*, 147–158.

(70) Walter, G; Hoppe, U; Vogel, J; Carl, G; Hartmann, P The Structure of Zinc Polyphosphate Glass Studied by Diffraction Methods and 31 P NMR. *Journal of non-crystalline solids* **2004**, *333*, 252–262.

(71) Edén, M. NMR Studies of Oxide-Based Glasses. *Annual Reports Section" C"(Physical Chemistry)* **2012**, *108*, 177–221.

(72) Zhang, J.; Spikes, H. On the Mechanism of ZDDP Antiwear Film Formation. *Tribology Letters* **2016**, *63*, 1–15.